
ReCo: Retrieve and Co-segment for Zero-shot Transfer

Gyungin Shin¹

¹Visual Geometry Group
University of Oxford
UK

Weidi Xie^{1,2}

²Coop. Medianet Innovation Center
Shanghai Jiao Tong University
China

Samuel Albanie³

³Department of Engineering
University of Cambridge
UK

Abstract

Semantic segmentation has a broad range of applications, but its real-world impact has been significantly limited by the prohibitive annotation costs necessary to enable deployment. Segmentation methods that forgo supervision can side-step these costs, but exhibit the inconvenient requirement to provide labelled examples from the target distribution to assign concept names to predictions. An alternative line of work in language-image pre-training has recently demonstrated the potential to produce models that can both assign names across large vocabularies of concepts and enable zero-shot transfer for classification, but do not demonstrate commensurate segmentation abilities.

In this work, we strive to achieve a synthesis of these two approaches that combines their strengths. We leverage the retrieval abilities of one such language-image pre-trained model, CLIP, to dynamically curate training sets from unlabelled images for arbitrary collections of concept names, and leverage the robust correspondences offered by modern image representations to co-segment entities among the resulting collections. The synthetic segment collections are then employed to construct a segmentation model (without requiring pixel labels) whose knowledge of concepts is inherited from the scalable pre-training process of CLIP. We demonstrate that our approach, termed **Retrieve and Co-segment (ReCo)** performs favourably to unsupervised segmentation approaches while inheriting the convenience of nameable predictions and zero-shot transfer. We also demonstrate ReCo's ability to generate specialist segmenters for extremely rare objects¹.

1 Introduction

The objective of *semantic segmentation* is to partition an image into coherent regions and to assign to each region a semantic label. This task has myriad applications across domains such as medical image analysis, autonomous driving, industrial process monitoring and wildlife tracking. However, there are several key challenges that have hindered the deployment of existing semantic segmentation approaches to date: (1) **Cost**: collecting manual pixel-level annotations is extraordinarily expensive (e.g. 90 minutes per image for high quality labels [14]), limiting the use of fully-supervised approaches; (2) **Flexibility**: supervised approaches have typically been trained with limited lists of pre-defined categories and lack the ability to recognise rare or novel categories (such as those described by free-form text); (3) **Complexity of deployment**: unsupervised segmentation methods have dramatically reduced annotation costs, but still exhibit the inconvenience of requiring labelled examples to assign names to predictions; (4) **Data access**: many existing approaches (both supervised and unsupervised) are trained on the *target data distribution*, requiring both that this distribution is known at training time (limiting flexibility) and that this data is accessible, which may not be the case for legal/ethical reasons (e.g. medical image data).

¹Project page: <https://www.robots.ox.ac.uk/~vgg/research/reco>

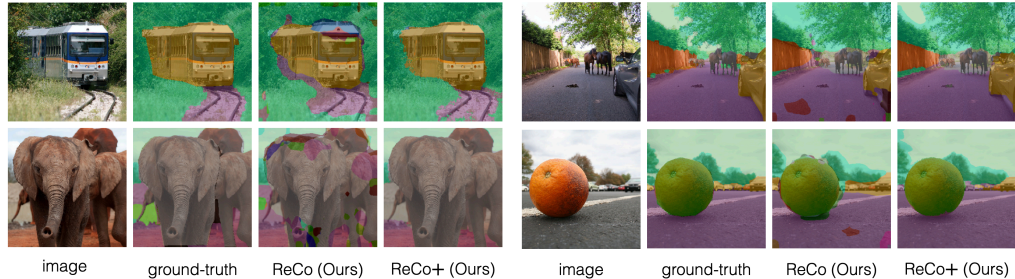


Figure 1: We propose ReCo, a new framework for semantic segmentation zero-shot transfer without pixel supervision. The figure depicts ReCo segmentations for COCO-Stuff [6], indicating promising results in the challenging zero-shot transfer setting. We also illustrate results with unsupervised adaptation to the target distribution (ReCo+), trading flexibility for improved segmentation quality.

There is a rich body of semantic segmentation literature that proposes solutions to subsets of these challenges, but to our knowledge no existing work addresses their full combination. To tackle all four challenges, we draw inspiration from two lines of recent research. The first line of research has shown that modern deep architectures (most notably vision transformers [17]) develop the ability to infer the spatial extent of objects without pixel supervision [7, 59, 80, 87, 78, 54] and moreover can establish semantically consistent correspondences across images [13, 24]. The second line of research has demonstrated that large-scale visual-language pre-training [72, 35] produces models that possess both a large vocabulary and remarkable *zero-shot transfer* potential—the ability to recognise concepts on target datasets without access to the target data distribution during training.

In this work, we target a synthesis of these two approaches that draws on their respective strengths for the semantic segmentation task. We first employ CLIP [72] to curate training sets from unlabelled images for any desired list of concepts. We then exploit the robust semantic correspondences offered by modern vision backbones to co-segment concepts among the resulting curated collections. Finally, we use these co-segmented concepts to construct a segmentation model for the given concepts, *without* requiring training. This framework, which we term **Retrieve and Co-segment (ReCo)**, performs favourably to existing unsupervised segmentation approaches while preserving the benefits of a wide vocabulary, named predictions and zero-shot transfer exemplified by CLIP.

Our contributions are three-fold: (1) We propose the ReCo framework, enabling open vocabulary semantic segmentation, without pixel annotations or the need to provide labelled examples from the target domain thereby enabling zero-shot transfer; (2) We compare our approach to prior work on standard semantic segmentation benchmarks (COCO-Stuff [6], Cityscapes [14], and KITTI-STEP [88]), and further illustrate the ability of ReCo to segment rare concepts beyond these benchmarks; (3) For cases when the target image distribution *is* available, we demonstrate that a simple extension of our approach, ReCo+, can exploit this data access via unsupervised adaptation to bring further gains.

2 Related work

Our work is connected to several themes in the literature, which we describe next.

Unsupervised semantic segmentation. There has been considerable recent progress towards unsupervised semantic segmentation with deep neural networks by leveraging ideas from self-supervised learning. Learning objectives based on maximising mutual information between views [34, 60], metric learning across proposals [94, 83], equivariance and invariance constraints [12], distillation of self-supervised feature correspondences [24] and cross modal cues (vision and LiDAR) [86] have all shown their potential for this task. One drawback of these approaches is a reliance on either nearest neighbour search on a held-out set with pixel level annotations or the Hungarian algorithm [45] (optimally matching predictions against ground-truth semantic masks) to produce segments with names. By contrast, ReCo is independent of labelled examples during both training and inference, simplifying deployment.

Weakly-supervised semantic segmentation. To reduce annotation costs, a number of works have explored weaker cues such eye tracking [63], pointing [4, 71, 11], sparse pixel labels [79], scribbles [49], web-queried samples [36], boxes [15, 42, 81], extreme clicks [64, 53], image-level labels [96, 89, 18, 1, 8, 67, 70] and free-form text [91]. However, such approaches still require the weak annotation to be attached to the data used to train the segmentation model—by contrast, ReCo can in

principle train a segmenter from any unlabelled collection of images. ReCo also bears a conceptual similarity with *webly-supervised* approaches [19] for semantic segmentation [36, 77]. These methods employ an image search engine such as Google to provide training samples for concepts. However, their flexibility is limited (this approach cannot be applied to private or commercially sensitive data, for example) and they lack the ability to leverage the knowledge of the search engine itself during inference (we demonstrate that integrating the vision-language model into the inference procedure brings significant gains in performance).

Zero-shot semantic segmentation with pretrained language/vision-language embeddings. A diverse body of work has explored zero-shot semantic segmentation, broadly defined as the task of segmenting categories for which no labels were provided during training (often termed *zero-label* semantic segmentation [90]). The key idea underlying many of these works is to leverage relationships encoded in pretrained word embeddings (such as word2vec [55] or GloVe [68]) to enable generalisation to unseen categories [95, 5, 23, 90, 40, 29, 47, 65]. More recent work has sought to leverage the vision-language embedding space learned by CLIP [72] to improve dense prediction in various settings [97, 73, 46, 92]. We adopt a variation of DenseCLIP [97] as a component of our framework. Additionally, differently from the above, we pursue the formulation of *zero-shot transfer* popularised by CLIP [72] which evaluates performance on *unseen datasets* rather than *unseen categories*. Consequently, unlike these works our model has no access to either labelled or unlabelled examples from the target data distribution (or pixel-level labels from the source distribution, as investigated by [92]). We note one exception: in addition to their primary zero-shot evaluations, DenseCLIP [97] also report an “annotation-free” evaluation without access to the target dataset—we compare our approach with theirs under an equivalent setting.

Large-vocabulary/rare concept segmenters. To scale up the number of concepts that can be segmented by a model several strategies based on captions [21], grounded text descriptions [39] and annotation transfer [30, 32] have been explored. In a differing direction, various losses and incremental learning techniques have been employed [31, 27] to better segment rare concepts. Unlike ReCo, however, each of the above approaches still requires costly pixel-level annotations.

Co-segmentation which aims to segment common regions among a collection of images, has been widely studied with classical computer vision approaches [74, 58, 84, 3, 38, 85]. The topic has been revisited with deep learning using shared encoder networks [9, 48, 2, 51], iterative refinement [93] and weak (class-label) supervision [28]. While ReCo can in principle make use of any unsupervised co-segmentation algorithm, we find that a simple correlation strategy works well, and thus we adopt it for our approach.

3 Method

In this section, we introduce the ReCo framework (Sec. 3.1) which enables zero-shot transfer for semantic segmentation with arbitrary categories. We describe a language-based gating mechanism to enhance segmentation quality (Sec. 3.2), and a pseudo-labelling scheme, ReCo+, that adapts to a target distribution using predictions from ReCo (Sec. 3.3).

3.1 Retrieve and Co-segment (ReCo)

The inputs to ReCo are a collection of unlabelled images, and a list of text descriptions of concepts to be segmented. Through a combination of *image retrieval* and *co-segmentation* across the image collection, ReCo constructs a segmenter for the given concepts on the fly. During *inference*, this segmenter is applied *without* fine-tuning to images from a target distribution of interest, thus supporting the zero-shot transfer. The interaction of these three stages is illustrated in Fig. 2 and discussed in more detail below.

Curating exemplars through image retrieval. The first hypothesis underpinning our approach is that it is possible to construct a sufficiently large and diverse unlabelled image collection that contains examples (or closely related examples) of any concept we wish to segment. We consider this hypothesis to be reasonable in light of the fact that recent research has produced a number of diverse datasets spanning billions of images [52, 22, 35, 76].

To make use of this hypothesis for segmentation, we employ a vision-language model to curate an archive of images for each concept of interest. In this work, we use CLIP [72], a model comprising

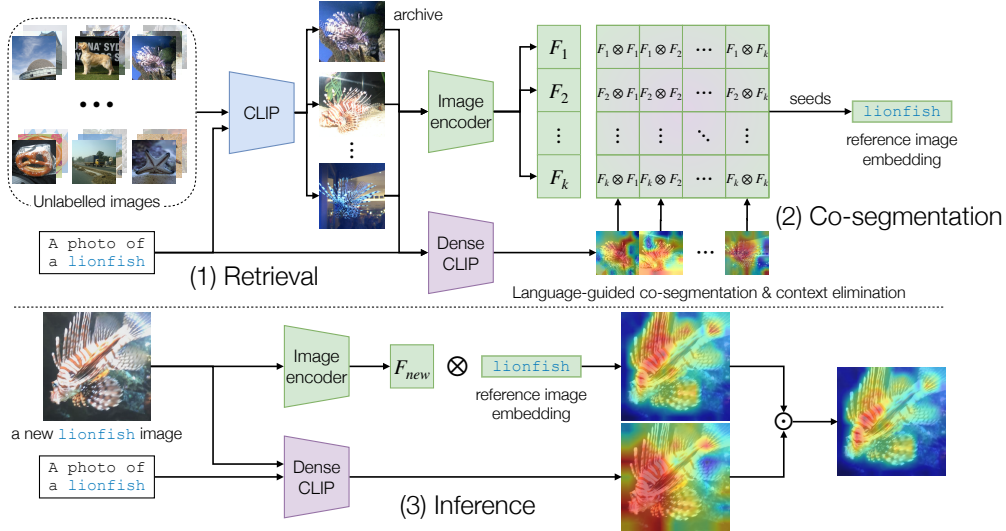


Figure 2: In this work, we propose ReCo, a framework for open vocabulary semantic segmentation zero-shot transfer. **Top:** (1) Given a large-scale unlabelled dataset and a category to segment, we first curate an archive of k images from the unlabelled collection using CLIP [72]. (2) Using a pre-trained visual encoder (e.g., MoCov2 [25], DeiT-S/16-SIN [59]), we extract dense features from the archive images, which are used to generate a reference image embedding for the given category via a co-segmentation process. **Bottom:** (3) During inference, the reference image is employed to produce an initial segmentation of the target concept which is refined with DenseCLIP. \otimes and \odot denote inner product and Hadamard product, respectively. See Sec. 3 for details.

an image encoder and a text encoder that enables efficient image retrieval for free-form text queries. In more detail, for a given text query describing a concept c the CLIP text encoder $\psi_{\mathcal{T}}$ produces an embedding $\psi_{\mathcal{T}}(c) \in \mathbb{R}^e$ which can be compared against the embeddings produced by the image encoder $\psi_{\mathcal{I}}$ for each image x in the unlabelled collection \mathcal{U} : $\{\psi_{\mathcal{I}}(x) \in \mathbb{R}^e : x \in \mathcal{U}\}$. We then build an archive from the k images that form nearest neighbours for each concept c . While a more sophisticated strategy (for instance, adjusting the archive size according to concept difficulty or prevalence) is possible with ReCo, we found that this simple approach worked well, and so we adopt it here. Note that, thanks to mature approximate nearest neighbour search techniques [37], this archive construction process can be readily applied to a collection \mathcal{U} containing billions of images.

Co-segmentation with seed pixels. The second hypothesis underpinning our approach is that modern vision-language models such as CLIP are capable of constructing archives of *high purity* (i.e. a high ratio of the archive images contain the concept of interest) provided that such exemplars exist in the underlying image collection \mathcal{U} (our first hypothesis). Our second hypothesis, which we validate through experiments in Sec. 4, enables the use of *co-segmentation* to obtain concept segments.

Concretely, given the k images comprising the archive for category c constructed by CLIP, we aim to segment regions corresponding to concepts that re-occur across the images. Since we expect the archive to be of high purity, and since modern visual backbones provide consistent semantic correspondences across images [24], we adopt a strategy of first identifying a *seed pixel* in each image that we are confident belongs to the target category, c . Intuitively, good seed pixels are ones that have close neighbours (i.e. strong support) across each of the archive images, since we assume that: (i) the target concept is common to all images in the archive, (ii) our visual backbone will produce consistent features for pixels belonging to the same concept. We then use these seed pixels to construct a reference embedding that can be used to classify pixels belonging to c .

In detail, we first extract dense features for each image in the archive using a pre-trained image encoder $\phi_{\mathcal{I}}$:

$$\{F_1, \dots, F_k\} = \{\phi_{\mathcal{I}}(x_1), \dots, \phi_{\mathcal{I}}(x_k)\} \quad (1)$$

where $F_i \in \mathbb{R}^{d \times h \times w}$ denotes (spatially) dense features for the i^{th} image with height h , width w and d channels. Each such feature is L2-normalised along its channel dimension.² Note that any image encoder $\phi_{\mathcal{I}}$ can be employed here (it need not be CLIP).

We identify seed pixels in four steps: First, we construct an adjacency matrix $A^{khw \times khw}$ among all features in the archive. Here, each of the $k \times k$ submatrices, $A_{ij} \in \mathbb{R}^{hw \times hw}$, encodes pairwise similarities between features from image i and image j for $i, j \in \{1, \dots, k\}$. Second, we aim to identify, for each pixel in the archive, the similarity of its nearest neighbour among each of the k images. To do so, we apply a `max` operator along the columns of each submatrix (reducing the hw columns of each submatrix to 1 and reducing the overall adjacency matrix dimensions to $khw \times k$). Third, we aim to identify the average *support* that each pixel has among the k archive images. For this, we apply a `mean` operator over the columns of each submatrix such that each row of the resulting $khw \times 1$ matrix encodes the mean maximum similarity across k images. Finally, we identify the seed pixel locations by applying an `argmax` operator to each of the k submatrices of size $hw \times 1$, yielding the spatial indices of the features in each image with highest average maximum similarity across the archive.

To construct a classifier for concept c , we simply average the embeddings of the k seed pixels from its archive and L2-normalise the resultant vector to produce the reference embedding $f_c \in \mathbb{R}^d$.

Inference. To localise instances of the category in a new image x_{new} , we first compute the dot-product between f_c and the L2-normalised dense features F_{new} from the new image, and pass the result through a sigmoid:

$$P_{\text{new}}^c = \sigma(f_c \cdot F_{\text{new}}) \in [0, 1]^{h \times w} \quad (2)$$

where P_{new}^c denotes an initial estimate of the probability map corresponding to category c .

To refine this probability map, we draw inspiration from recent work [97, 73] showing that dense visual CLIP features can be usefully correlated against a given CLIP text embedding. Concretely, we employ the DenseCLIP mechanism of Zhou et al. [97] to highlight regions of the input that are salient for the target category c as follows. For image x_{new} , we extract features $V_{\text{new}} \in \mathbb{R}^{e_v \times h \times w}$ from the last self-attention layer values of the CLIP image encoder (here e_v denotes the value feature dimension), project the features into the joint space \mathbb{R}^e with the CLIP image encoder’s final linear projection and L2-normalise the result. We then compute the CLIP text embedding $\psi_{\mathcal{T}}(c) \in \mathbb{R}^e$ for the target concept c and L2-normalise it before producing a saliency map $\mathcal{S}_{\text{new}}^c \in [0, 1]^{h \times w}$ by applying the text embedding as a 1×1 convolution to the visual features and applying a sigmoid activation function to the result. Note that our use of a sigmoid activation function differs from the softmax used by [97], since we process each concept independently.

Our final probability map for category c is produced by the Hadamard product of these estimates:

$$\bar{P}_{\text{new}}^c = P_{\text{new}}^c \odot \mathcal{S}_{\text{new}}^c \quad (3)$$

In case of multiple categories predictions, we concatenate all the category prediction maps and apply `argmax` to the category dimension. As a post-processing step, we also experiment with the effect of applying a CRF [44] as a simple post-processing step (similarly to [24]). Pseudocode for ReCo can be found in Appendix B.

3.2 Language-guided co-segmentation and context elimination

Even when an archive has high purity, co-segmenting the target concept c from the collection of images can be challenging due to the potential presence of distractor categories \tilde{c} that often co-occur with c . For example, *cars* often co-occur with *roads* and likewise *aeroplanes* with *sky*. To minimise the risk of the co-segmentation algorithm anchoring on unintended categories, we introduce two mechanisms into the co-segmentation procedure, namely, *language-guided co-segmentation* and *context elimination*.

Language-guided co-segmentation. Specifically, for each x_i in the archive, we first compute the corresponding saliency map $\mathcal{S}_i^c \in [0, 1]^{h \times w}$ using DenseCLIP. We then vectorise this map and use it to filter the co-segmentation similarities by replacing each row of $A_{j,i}$ with the Hadamard product of itself with $\text{vec}(\mathcal{S}_i^c) \in [0, 1]^{1 \times hw}$ (where $\text{vec}(\cdot)$ denotes vectorisation) for each submatrix

²For clarity purposes, we assume that all images share the same spatial extent (and thus their dense features also do). However, the proposed co-segmentation approach can be applied to images with different resolutions.

$j = \{1, \dots, k\}$. Intuitively, this serves to act as a *gate* that preserves similarities only for pixels identified by CLIP as salient for the target concept.

Context elimination. To reduce the influence of widely co-occurring distractors, we select a few common background categories \tilde{c} that frequently appear in images (e.g., *tree*, *sky*, *road*) and compute their reference embeddings $f_{\tilde{c}}$ as described in the seeding procedure of Sec. 3.1. We then use the resulting attention maps $P_i^{\tilde{c}}$ produced by these reference embeddings to suppress regions of common background context in the subsequent co-segmentation processes for different categories. This is done similarly as above, by vectorising and replacing each row of $A_{j,i}$ with the Hadamard product of itself with $\text{vec}(1 - P_i^{\tilde{c}}) \in [0, 1]^{1 \times hw}$ for each submatrix $j = \{1, \dots, k\}$. If a target concept c is identical to one of the common background categories \tilde{c} , we replace f_c with the corresponding $f_{\tilde{c}}$.

3.3 ReCo+: Fine-tuning ReCo with pseudo-labels

The ReCo framework outlined above requires no training and no access to the target distribution. However, it is possible to consider a simple extension to this idea when access to the target image distribution is available. Our proposed extension, ReCo+, simply trains a segmentation architecture (e.g., DeepLabv3+ [10]) with the segmentation masks from ReCo as pseudo-masks.

4 Experiments

In this section, we start by describing the datasets used for our experiments (Sec. 4.1) and implementation details (Sec. 4.2). Then, we conduct an ablation study (Sec. 4.3) and compare our model to state-of-the-art methods for unsupervised semantic segmentation (Sec. 4.4). Finally, we showcase our model’s ability to segment rare-category objects (Sec. 4.5) and discuss limitations (Sec. 4.6).

4.1 Datasets

For our ablation study, we use the ImageNet1K [16] validation set to curate archive for concepts of interest. The dataset covers 1K classes with 50 images for each class. To measure segmentation performance in the zero-shot transfer setting, we use the PASCAL-Context [57] validation set for evaluation, which has 5,104 images of 59 categories excluding the background class.

To compare with previous unsupervised segmentation methods, we use the ImageNet1K training set to construct the reference embedding for the concept we wish to segment. The dataset has 1K classes with 1.2M images. We evaluate on standard benchmarks including the Cityscapes [14] validation split, which has 500 urban scene images of 27 categories, KITTI-STEP [88] validation set, which is composed of 2,981 urban scene images of 19 categories, and COCO-Stuff [6] validation split, which has 4,172 images of 171 low-level thing and stuff categories excluding background class. Following [12, 24], we use the 27 mid-level categories for evaluation. For unsupervised adaptation with ReCo+ (Sec. 3.1), we train on ReCo pseudo-labels on the Cityscapes training set with 2,975 images, KITTI-STEP training set which contains 5,027 images, and the COCO-Stuff10K subset which has 9,000 images for each respective benchmark. We emphasize that *no ground-truth labels are used for training*.

Finally, to demonstrate our model’s ability to segment rare concepts, we use the LAION-5B dataset [76] with 5 billion images as a large collection of images that we expect to satisfy our first hypothesis, namely that it will have coverage of rare concepts. To assess performance, we use the FireNet dataset [62] which has 1,452 images spanning rare fire safety-related classes. For our experiment, we select the *fire extinguisher* class as an example of a concept that is important but rare in vision datasets (it is not contained in ImageNet1K [75], for example) and evaluate ReCo on 263 images containing at least one instance of the category. As a further proof of concept, we also demonstrate co-segmentations of the *Antikythera mechanism* (a historical item that does not appear in WordNet [56], or any labelled vision datasets that we are aware of).

4.2 Implementation details

Here, we describe the hyperparameters used to train ReCo+, inference details and evaluation metrics. Our implementation is based on the PyTorch library [66] and will be made publicly available.

ReCo+ Training. While ReCo does not require training, we train ReCo+ based on the DeepLabv3+ [10] segmentation architecture with a ResNet101 [26] backbone on the predictions from ReCo as described in 3.1. All training images are resized and center-cropped to 320×320 pixels and data augmentations such as random scaling, cropping, and horizontal flipping are applied with

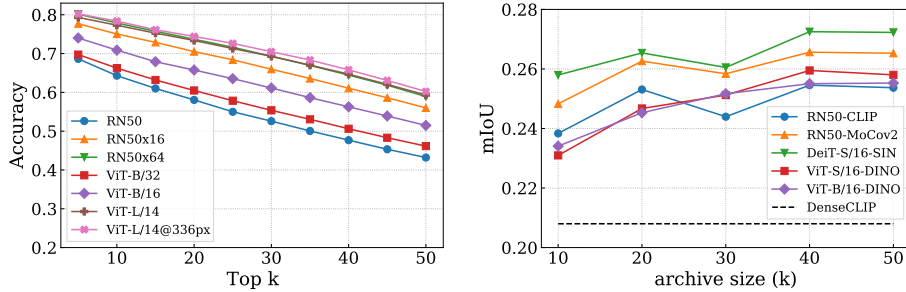


Figure 3: **Ablation studies.** **Left:** Image retrieval performance of different CLIP models on the ImageNet1K validation set with k ranging from 5 to 50. ViT-L/14@336px performs particularly strongly, suggesting the ability to curate archives of high purity. **Right:** Co-segmentation performance on PASCAL-Context validation set as we vary the archive size and choice of visual encoders. We observe a general trend towards improved performance with increasing archive size for all encoders.

random color jittering and Gaussian blurring. We use the Adam optimiser [43] with an initial learning rate of 5×10^{-4} and a weight decay of 2×10^{-4} with the Poly learning rate schedule as in [50, 10]. Training consists of 20K gradient iterations with a batch size of 8 and takes about 5 hours on a single 24GB NVIDIA P40 GPU.

Inference. Whenever DenseCLIP is employed, we use the ResNet50x16 model (following [97]) to construct a saliency map for each image. For the COCO-Stuff and Cityscapes benchmarks, we resize and center crop the input images to 320×320 pixels as in [24]. For the KITTI-STEP validation set, we use the original resolution of each image as in [41]. For the FireNet benchmark, we resize the shorter side of images to 512 pixels and predict a single class of *fire extinguisher* by thresholding the predicted heatmap with probability of 0.5.

Evaluation metrics. Following the common practice [34, 12, 24], we report pixel accuracy (Acc.) and mean intersection-over-union (mIoU).

4.3 Ablation studies

Ability of CLIP to curate archives. We begin by assessing the validity of our second hypothesis—namely that CLIP is capable of achieving *high purity* archives from unlabelled images. To this end, we evaluate the retrieval performance of different CLIP models on the ImageNet1K validation set when constructing different archive sizes. In detail, for each archive size, k , we compute the precision of the top- k retrieved images based on whether the the ground-truth image-labels match the query text. As can be seen in Fig. 3 (left), all CLIP models achieve solid retrieval performance, suggesting their potential for curating high purity archives as part of ReCo. Since ViT-L/14@336px performs best, we employ this as our retrieval model in the remaining experiments.

DenseCLIP	LGC	CE	CRF	Acc.	mIoU
✗	✗	✗	✗	16.8	5.7
✓	✗	✗	✗	41.1	21.8
✓	✓	✗	✗	43.1	23.1
✓	✗	✓	✗	49.7	26.0
✓	✓	✓	✗	50.9	26.6
✓	✓	✓	✓	51.6	27.2

Table 1: **Influence of ReCo components for zero-shot transfer on PASCAL-Context [57].** We observe that integrating DenseCLIP during inference, *Language-guided co-segmentation* (LGC), *Context elimination* (CE), and CRF [44] post-processing each contribute to improved performance. All comparisons use a DeiT-SIN visual backbone for co-segmentation and ViT-L/14@336px for archive curation.

Influence of archive size and visual encoder used for co-segmentation. In Fig. 3 (right) we illustrate the effect of using different pre-trained architectures, *e.g.* MoCov2 [25], DINO [7], CLIP [72], DeiT-SIN [59], as the archive size (and thus the number of images used for co-segmentation) changes. The y-axis depicts segmentation performance for ReCo with these configurations on the PASCAL-Context benchmark. We observe that using larger archives tends to improve performance (likely due to their reasonably high purity) albeit non-monotonically, and that features from DeiT-SIN

Model	Acc.	mIoU	Model	Acc.	mIoU	Model	Acc.	mIoU
Zero-shot transfer			Zero-shot transfer			Zero-shot transfer		
DenseCLIP [97]	32.2	19.6	DenseCLIP [97]	35.9	10.0	DenseCLIP [97]	34.1	15.3
ReCo (Ours)	46.1	26.3	MDC† [12]	-	7.0	ReCo (Ours)	70.6	29.8
Unsupervised adaptation			Unsupervised adaptation			Unsupervised adaptation		
IIC [34]	21.8	6.7	PiCIE† [12]	-	9.7	SegSort [33]	69.8	19.2
MDC [12]	32.2	9.8	D&S† [86]	-	16.2	HSG [41]	73.8	21.7
PiCIE [12]	48.1	13.8	ReCo (Ours)	74.6	19.3	ReCo+ (Ours)	75.3	31.9
PiCIE + H [12]	50.0	14.4	Unsupervised adaptation					
STEGO [24]	56.9	28.2	IIC [34]	47.9	6.4			
ReCo+ (Ours)	54.1	32.6	MDC [12]	40.7	7.1			
			PiCIE [12]	65.5	12.3			
			STEGO [24]	73.2	21.0			
			ReCo+ (Ours)	83.7	24.2			

Table 2: **Comparison to state-of-the-art approaches on COCO-Stuff (left), Cityscapes (middle), and KITTI-STEP (right) validation sets.** †Models trained on Waymo Open [82] and evaluated at the original resolution (reported from [86]). The best score for each metric under each protocol is highlighted in **bold**. We observe that ReCo and ReCo+ perform strongly relative to prior work under zero-shot transfer and unsupervised adaptation protocols, respectively.

perform best. We therefore use DeiT-SIN with an archive size of $k=50$ for the remaining experiments otherwise stated.

Influence of ReCo framework components. We next assess the effect of employing DenseCLIP during inference, the *language-guided co-segmentation* and *context elimination* components of ReCo which seek to improve the quality of co-segmentation achieved across each archive to boost downstream segmentation performance. When applying context elimination, we select *tree*, *sky*, *building*, *road*, and *person* as common background concepts appearing in natural images to be suppressed. In Tab. 1, we show the effect of three of these strategies, together with the effect of applying a CRF [44] as post-processing. We observe that integrating DenseCLIP into the inference procedure brings a significant gain in performance which we believe is driven by the notable robustness of CLIP features under zero-shot transfer [72]. In addition, language-guided co-segmentation and context elimination further boost co-segmentation performance, while the CRF brings a small gain. We therefore use each of these strategies (including CRF post-processing) in the remaining experiments.

4.4 Comparison to state-of-the-art unsupervised methods

We compare ReCo and ReCo+ to state-of-the-art unsupervised semantic segmentation models on standard benchmarks, including COCO-Stuff [6], Cityscapes [14] and KITTI-STEP [88] under both zero-shot transfer and unsupervised adaptation (training without labels on the target distribution). For COCO-Stuff, we observe that the mid-level categories used for evaluation are somewhat abstract for retrieval (for instance, one mid-level category is “outdoor objects”, which may include many low-level categories beyond the target hierarchy). To avoid introducing ambiguity to the co-segmentation procedure, we instead directly use the low-level categories and then merge the predictions into the mid-level categories. Additionally, we rephrase two category names to reduce ambiguity (*parking to parking lot* and *vegetation to tree*) in Cityscapes and KITTI-STEP based on the descriptions found in [14]. A detailed discussion can be found in Appendix C.2.

As shown in Tab. 2, ReCo strongly outperforms prior models on all benchmarks for zero-shot transfer. Under an unsupervised adaptation protocol, ReCo+ outperforms the state-of-the-art by a large margin on the Cityscapes and KITTI-STEP. On COCO-Stuff, ReCo+ achieves slightly lower pixel accuracy compared to [24] but a considerably higher mIoU. In Fig. 1, we visualise the sample predictions of our models on the COCO-Stuff.

4.5 Segmenting rare concepts

By virtue of inheriting CLIP’s diverse knowledge of nameable visual concepts, ReCo exhibits the ability to segment rare categories. We first demonstrate this ability for *fire extinguisher* objects, which have important fire-safety implications but seldom appear in popular semantic segmentation benchmarks. To assess performance, we evaluate segmentation quality on the FireNet dataset (as described in Sec. 4.1) and achieve reasonable performance on pixel accuracy (93.3) and IoU (44.9)

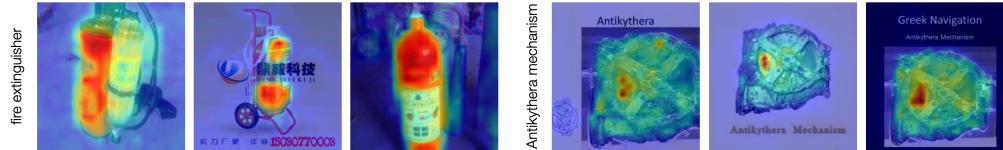


Figure 4: **Co-segmentations of rare concepts.** **Left:** *fire extinguisher*. **Right:** *Antikythera mechanism*. We show selected samples from ReCo archives for each concept, together with their co-segmentations. In each cases, ReCo successfully identifies the regions associated with the concept.

metrics. In Fig. 4 (left) we visualise the co-segmentation produced by ReCo across sample images container fire extinguishers. As an additional demonstration (Fig. 4, right), we also show co-segmentations for images containing the views of the (unique) *Antikythera mechanism*. In both cases, we observe that ReCo is capable of co-segmenting the concept of interest without labelled examples.

4.6 Limitations

Our work has several limitations: (1) There may be cases for which our first hypothesis does not hold—concepts so rare that they do not appear in billion-image scale datasets. In such cases, *e.g.* “a purple elephant with square orange feet wearing an inverted cowboy hat in front of the Doge’s Palace”, ReCo will struggle. (2) We make use of CLIP (a computationally heavy model) during inference. Future work could address this with pruning and hardware optimisation strategies. (3) We employ ImageNet as the unlabelled image collection for our primary investigations, which is known to exhibit an object-centric bias. While qualitative results suggest that ReCo can learn from extremely diverse data [76], a more comprehensive empirical evaluation would strengthen this result. (4) Models like CLIP are expensive to train and are consequently updated infrequently. If a new concept emerges (*e.g.* a new product) after CLIP was trained, ReCo will be unable to build an archive to enable co-segmentation for this concept. (5) Although our work is zero-shot in the sense that it is not trained on the target distribution, we still use of a subset of the target data distribution (primarily through ablations on PASCAL-Context) to guide the development of our method. As a result, our design likely contains choices that subtly favour performance on the evaluation tasks.

5 Conclusion

In this work, we introduced the ReCo framework for semantic segmentation zero-shot transfer. By drawing on the strengths of large-scale language-image pre-training and modern visual backbones, ReCo attains the ability to segment rare concepts and to directly assign names to concepts without labelled examples from the target distribution. In addition, experimental comparisons demonstrate that ReCo strongly outperforms existing zero-shot transfer approaches that forgo pixel supervision.

6 Acknowledgements

GS is supported by AI Factory, Inc. in Korea. GS would like to thank Yash Bhalgat, Tengda Han, Charig Yang, Guanqi Zhan, and Chuhan Zhang for proof-reading. SA would like to acknowledge the support of Z. Novak and N. Novak in enabling his contribution.

References

- [1] Jiwoon Ahn and Suha Kwak. Learning pixel-level semantic affinity with image-level supervision for weakly supervised semantic segmentation. In *CVPR*, 2018.
- [2] Sayan Banerjee, Avik Hati, Subhasis Chaudhuri, and Rajbabu Velmurugan. Cosegnet: Image co-segmentation using a conditional siamese convolutional network. In *IJCAI*, 2019.
- [3] Dhruv Batra, Adarsh Kowdle, Devi Parikh, Jiebo Luo, and Tsuhan Chen. icoseg: Interactive co-segmentation with intelligent scribble guidance. In *CVPR*, 2010.
- [4] Amy Bearman, Olga Russakovsky, Vittorio Ferrari, and Li Fei-Fei. What’s the point: Semantic segmentation with point supervision. In *ECCV*, 2016.
- [5] Maxime Bucher, Tuan-Hung Vu, Mathieu Cord, and Patrick Pérez. Zero-shot semantic segmentation. In *NeurIPS*, 2019.
- [6] Holger Caesar, Jasper Uijlings, and Vittorio Ferrari. Coco-stuff: Thing and stuff classes in context. In *CVPR*, 2018.
- [7] Mathilde Caron, Hugo Touvron, Ishan Misra, Hervé Jégou, Julien Mairal, Piotr Bojanowski, and Armand Joulin. Emerging properties in self-supervised vision transformers. In *ICCV*, 2021.

- [8] Yu-Ting Chang, Qiaosong Wang, Wei-Chih Hung, Robinson Piramuthu, Yi-Hsuan Tsai, and Ming-Hsuan Yang. Weakly-supervised semantic segmentation via sub-category exploration. In *CVPR*, 2020.
- [9] Hong Chen, Yifei Huang, and Hideki Nakayama. Semantic aware attention based deep object co-segmentation. In *ACCV*, 2018.
- [10] Liang-Chieh Chen, Yukun Zhu, George Papandreou, Florian Schroff, and Hartwig Adam. Encoder-decoder with atrous separable convolution for semantic image segmentation. In *ECCV*, 2018.
- [11] Bowen Cheng, Omkar Parkhi, and Alexander Kirillov. Pointly-supervised instance segmentation. *arXiv:2104.06404*, 2021.
- [12] Jang Hyun Cho, Utkarsh Mall, Kavita Bala, and Bharath Hariharan. Picie: Unsupervised semantic segmentation using invariance and equivariance in clustering. In *CVPR*, 2021.
- [13] Edo Collins, Radhakrishna Achanta, and Sabine Susstrunk. Deep feature factorization for concept discovery. In *ECCV*, 2018.
- [14] Marius Cordts, Mohamed Omran, Sebastian Ramos, Timo Rehfeld, Markus Enzweiler, Rodrigo Benenson, Uwe Franke, Stefan Roth, and Bernt Schiele. The cityscapes dataset for semantic urban scene understanding. In *CVPR*, 2016.
- [15] Jifeng Dai, Kaiming He, and Jian Sun. Boxesup: Exploiting bounding boxes to supervise convolutional networks for semantic segmentation. In *ICCV*, 2015.
- [16] Jia Deng, Wei Dong, Richard Socher, Li-Jia Li, Kai Li, and Li Fei-Fei. Imagenet: A large-scale hierarchical image database. In *CVPR*, 2009.
- [17] Alexey Dosovitskiy, Lucas Beyer, Alexander Kolesnikov, Dirk Weissenborn, Xiaohua Zhai, Thomas Unterthiner, Mostafa Dehghani, Matthias Minderer, Georg Heigold, Sylvain Gelly, Jakob Uszkoreit, and Neil Houlsby. An image is worth 16x16 words: Transformers for image recognition at scale. In *ICLR*, 2021.
- [18] Ruo Chen Fan, Qibin Hou, Ming-Ming Cheng, Gang Yu, Ralph R. Martin, and Shi-Min Hu. Associating inter-image salient instances for weakly supervised semantic segmentation. In *ECCV*, 2018.
- [19] Robert Fergus, Li Fei-Fei, Pietro Perona, and Andrew Zisserman. Learning object categories from google’s image search. In *ICCV*, 2005.
- [20] Robert Geirhos, Patricia Rubisch, Claudio Michaelis, Matthias Bethge, Felix A. Wichmann, and Wieland Brendel. Imagenet-trained CNNs are biased towards texture; increasing shape bias improves accuracy and robustness. In *ICLR*, 2019.
- [21] Golnaz Ghiasi, Xiuye Gu, Yin Cui, and Tsung-Yi Lin. Open-vocabulary image segmentation. *arXiv:2112.12143*, 2021.
- [22] Priya Goyal, Quentin Duval, Isaac Seessel, Mathilde Caron, Mannat Singh, Ishan Misra, Levent Sagun, Armand Joulin, and Piotr Bojanowski. Vision models are more robust and fair when pretrained on uncurated images without supervision. *arXiv:2202.08360*, 2022.
- [23] Zhangxuan Gu, Siyuan Zhou, Li Niu, Zihan Zhao, and Liqing Zhang. Context-aware feature generation for zero-shot semantic segmentation. In *ACM MM*, 2020.
- [24] Mark Hamilton, Zhoutong Zhang, Bharath Hariharan, Noah Snavely, and William T. Freeman. Unsupervised semantic segmentation by distilling feature correspondences. In *ICLR*, 2022.
- [25] Kaiming He, Haoqi Fan, Yuxin Wu, Saining Xie, and Ross Girshick. Momentum contrast for unsupervised visual representation learning. In *CVPR*, 2020.
- [26] Kaiming He, Xiangyu Zhang, Shaoqing Ren, and Jian Sun. Deep residual learning for image recognition. In *CVPR*, 2016.
- [27] Yin-Yin He, Peizhen Zhang, Xiu-Shen Wei, Xiangyu Zhang, and Jian Sun. Relieving long-tailed instance segmentation via pairwise class balance. *arXiv:2201.02784*, 2022.
- [28] Kuang-Jui Hsu, Yen-Yu Lin, Yung-Yu Chuang, et al. Co-attention cnns for unsupervised object co-segmentation. In *IJCAI*, 2018.
- [29] Ping Hu, Stan Sclaroff, and Kate Saenko. Uncertainty-aware learning for zero-shot semantic segmentation. *NeurIPS*, 2020.
- [30] Ronghang Hu, Piotr Dollár, Kaiming He, Trevor Darrell, and Ross Girshick. Learning to segment every thing. In *CVPR*, 2018.
- [31] Xinting Hu, Yi Jiang, Kaihua Tang, Jingyuan Chen, Chunyan Miao, and Hanwang Zhang. Learning to segment the tail. In *CVPR*, 2020.
- [32] Dat Huynh, Jason Kuen, Zhe Lin, Jiuxiang Gu, and Ehsan Elhamifar. Open-vocabulary instance segmentation via robust cross-modal pseudo-labeling. *arXiv:2111.12698*, 2021.
- [33] Jyh-Jing Hwang, Stella X Yu, Jianbo Shi, Maxwell D Collins, Tien-Ju Yang, Xiao Zhang, and Liang-Chieh Chen. Segsort: Segmentation by discriminative sorting of segments. In *ICCV*, 2019.
- [34] Xu Ji, João F Henriques, and Andrea Vedaldi. Invariant information clustering for unsupervised image classification and segmentation. In *ICCV*, 2019.
- [35] Chao Jia, Yinfei Yang, Ye Xia, Yi-Ting Chen, Zarana Parekh, Hieu Pham, Quoc Le, Yun-Hsuan Sung, Zhen Li, and Tom Duerig. Scaling up visual and vision-language representation learning with noisy text supervision. In *ICML*, 2021.
- [36] Bin Jin, Maria V Ortiz Segovia, and Sabine Susstrunk. Webly supervised semantic segmentation. In *CVPR*, 2017.
- [37] Jeff Johnson, Matthijs Douze, and Hervé Jégou. Billion-scale similarity search with gpus. *IEEE Transactions on Big Data*, 2019.
- [38] Armand Joulin, Francis Bach, and Jean Ponce. Discriminative clustering for image co-segmentation. In *CVPR*, 2010.

- [39] Aishwarya Kamath, Mannat Singh, Yann LeCun, Gabriel Synnaeve, Ishan Misra, and Nicolas Carion. Mdetr-modulated detection for end-to-end multi-modal understanding. In *ICCV*, 2021.
- [40] Naoki Kato, Toshihiko Yamasaki, and Kiyoharu Aizawa. Zero-shot semantic segmentation via variational mapping. In *ICCVW*, 2019.
- [41] Tsung-Wei Ke, Jyh-Jing Hwang, Yunhui Guo, Xudong Wang, and Stella X. Yu. Unsupervised hierarchical semantic segmentation with multiview cosegmentation and clustering transformers. In *CVPR*, 2022.
- [42] Anna Khoreva, Rodrigo Benenson, Jan Hosang, Matthias Hein, and Bernt Schiele. Simple does it: Weakly supervised instance and semantic segmentation. In *CVPR*, 2017.
- [43] Diederik P. Kingma and Jimmy Ba. Adam: A method for stochastic optimization. In *ICLR*, 2015.
- [44] Philipp Krähenbühl and Vladlen Koltun. Efficient inference in fully connected crfs with gaussian edge potentials. In *NeurIPS*, 2011.
- [45] Harold W. Kuhn. The Hungarian Method for the Assignment Problem. *Naval Research Logistics Quarterly*, 1955.
- [46] Boyi Li, Kilian Q Weinberger, Serge Belongie, Vladlen Koltun, and Rene Ranftl. Language-driven semantic segmentation. In *ICLR*, 2022.
- [47] Peike Li, Yunchao Wei, and Yi Yang. Consistent structural relation learning for zero-shot segmentation. *NeurIPS*, 2020.
- [48] Weihao Li, Omid Hosseini Jafari, and Carsten Rother. Deep object co-segmentation. In *ACCV*, 2019.
- [49] Di Lin, Jifeng Dai, Jiaya Jia, Kaiming He, and Jian Sun. Scribblesup: Scribble-supervised convolutional networks for semantic segmentation. In *CVPR*, 2016.
- [50] Wei Liu, Andrew Rabinovich, and Alexander C. Berg. ParseNet: Looking Wider to See Better. *arXiv:1506.04579*, 2015.
- [51] Weide Liu, Chi Zhang, Guosheng Lin, and Fayao Liu. Crnet: Cross-reference networks for few-shot segmentation. In *CVPR*, 2020.
- [52] Dhruv Mahajan, Ross Girshick, Vignesh Ramanathan, Kaiming He, Manohar Paluri, Yixuan Li, Ashwin Bharambe, and Laurens Van Der Maaten. Exploring the limits of weakly supervised pretraining. In *ECCV*, 2018.
- [53] Kevis-Kokitsi Maninis, Sergi Caelles, Jordi Pont-Tuset, and Luc Van Gool. Deep extreme cut: From extreme points to object segmentation. In *CVPR*, 2018.
- [54] Luke Melas-Kyriazi, Christian Rupprecht, Iro Laina, and Andrea Vedaldi. Deep spectral methods: A surprisingly strong baseline for unsupervised semantic segmentation and localization. *arXiv:2205.07839*, 2022.
- [55] Tomas Mikolov, Kai Chen, Greg Corrado, and Jeffrey Dean. Efficient estimation of word representations in vector space. *arXiv:1301.3781*, 2013.
- [56] George A Miller. Wordnet: a lexical database for english. *Communications of the ACM*, 1995.
- [57] Roozbeh Mottaghi, Xianjie Chen, Xiaobai Liu, Nam-Gyu Cho, Seong-Whan Lee, Sanja Fidler, Raquel Urtasun, and Alan Yuille. The role of context for object detection and semantic segmentation in the wild. In *CVPR*, 2014.
- [58] Lopamudra Mukherjee, Vikas Singh, and Charles R Dyer. Half-integrality based algorithms for cosegmentation of images. In *CVPR*, 2009.
- [59] Muzammal Naseer, Kanchana Ranasinghe, Salman Khan, Munawar Hayat, Fahad Khan, and Ming-Hsuan Yang. Intriguing properties of vision transformers. In *NeurIPS*, 2021.
- [60] Yassine Ouali, Céline Hudelot, and Myriam Tami. Autoregressive unsupervised image segmentation. In *ECCV*, 2020.
- [61] Yassine Ouali, Celine Hudelot, and Myriam Tami. Semi-supervised semantic segmentation with cross-consistency training. In *CVPR*, 2020.
- [62] Fabio Panella, Victor Melatti, and Jan Boehm. Firenet dataset. <http://www.firenet.xyz>. Accessed: 2022-05-17.
- [63] Dim P Papadopoulos, Alasdair DF Clarke, Frank Keller, and Vittorio Ferrari. Training object class detectors from eye tracking data. In *ECCV*, 2014.
- [64] Dim P Papadopoulos, Jasper RR Uijlings, Frank Keller, and Vittorio Ferrari. Extreme clicking for efficient object annotation. In *ICCV*, 2017.
- [65] Giuseppe Pastore, Fabio Cermelli, Yongqin Xian, Massimiliano Mancini, Zeynep Akata, and Barbara Caputo. A closer look at self-training for zero-label semantic segmentation. In *CVPR*, 2021.
- [66] Adam Paszke, Sam Gross, Francisco Massa, Adam Lerer, James Bradbury, Gregory Chanan, Trevor Killeen, Zeming Lin, Natalia Gimelshein, Luca Antiga, Alban Desmaison, Andreas Kopf, Edward Yang, Zachary DeVito, Martin Raison, Alykhan Tejani, Sasank Chilamkurthy, Benoit Steiner, Lu Fang, Junjie Bai, and Soumith Chintala. Pytorch: An imperative style, high-performance deep learning library. In *NeurIPS*, 2019.
- [67] Deepak Pathak, Philipp Krahenbuhl, and Trevor Darrell. Constrained convolutional neural networks for weakly supervised segmentation. In *ICCV*, 2015.
- [68] Jeffrey Pennington, Richard Socher, and Christopher D Manning. Glove: Global vectors for word representation. In *EMNLP*, 2014.
- [69] Hieu Pham, Zihang Dai, Golnaz Ghiasi, Hanxiao Liu, Adams Wei Yu, Minh-Thang Luong, Mingxing Tan, and Quoc V Le. Combined scaling for zero-shot transfer learning. *arXiv:2111.10050*, 2021.
- [70] Pedro O Pinheiro and Ronan Collobert. From image-level to pixel-level labeling with convolutional networks. In *CVPR*, 2015.

- [71] Rui Qian, Yunchao Wei, Honghui Shi, Jiachen Li, Jiaying Liu, and Thomas Huang. Weakly supervised scene parsing with point-based distance metric learning. In *AAAI*, 2019.
- [72] Alec Radford, Jong Wook Kim, Chris Hallacy, Aditya Ramesh, Gabriel Goh, Sandhini Agarwal, Girish Sastry, Amanda Askell, Pamela Mishkin, Jack Clark, Gretchen Krueger, and Ilya Sutskever. Learning transferable visual models from natural language supervision. In *ICML*, 2021.
- [73] Yongming Rao, Wenliang Zhao, Guangyi Chen, Yansong Tang, Zheng Zhu, Guan Huang, Jie Zhou, and Jiwen Lu. Densclip: Language-guided dense prediction with context-aware prompting. *arXiv:2112.01518*, 2021.
- [74] Carsten Rother, Tom Minka, Andrew Blake, and Vladimir Kolmogorov. Cosegmentation of image pairs by histogram matching-incorporating a global constraint into mrfs. In *CVPR*, 2006.
- [75] Olga Russakovsky, Jia Deng, Hao Su, Jonathan Krause, Sanjeev Satheesh, Sean Ma, Zhiheng Huang, Andrej Karpathy, Aditya Khosla, Michael Bernstein, et al. Imagenet large scale visual recognition challenge. *IJCV*, 2015.
- [76] Christoph Schuhmann, Richard Vencu, Romain Beaumont, Theo Coombes, Cade Gordon, Aarush Katta, Robert Kaczmarczyk, and Jenia Jitsev. LAION-5B: laion-5b: A new era of open large-scale multi-modal datasets. <https://laion.ai/laion-5b-a-new-era-of-open-large-scale-multi-modal-datasets/>, 2022.
- [77] Tong Shen, Guosheng Lin, Chunhua Shen, and Ian Reid. Bootstrapping the performance of webly supervised semantic segmentation. In *CVPR*, 2018.
- [78] Gyungin Shin, Samuel Albanie, and Weidi Xie. Unsupervised salient object detection with spectral cluster voting. In *CVPRW*, 2022.
- [79] Gyungin Shin, Weidi Xie, and Samuel Albanie. All you need are a few pixels: semantic segmentation with pixelpick. In *ICCVW*, 2021.
- [80] Oriane Siméoni, Gilles Puy, Huy V Vo, Simon Roburin, Spyros Gidaris, Andrei Bursuc, Patrick Pérez, Renaud Marlet, and Jean Ponce. Localizing objects with self-supervised transformers and no labels. *arXiv:2109.14279*, 2021.
- [81] Chunfeng Song, Yan Huang, Wanli Ouyang, and Liang Wang. Box-driven class-wise region masking and filling rate guided loss for weakly supervised semantic segmentation. In *CVPR*, 2019.
- [82] Pei Sun, Henrik Kretzschmar, Xerxes Dotiwalla, Aurelien Chouard, Vijaysai Patnaik, Paul Tsui, James Guo, Yin Zhou, Yuning Chai, Benjamin Caine, Vijay Vasudevan, Wei Han, Jiquan Ngiam, Hang Zhao, Aleksei Timofeev, Scott Ettinger, Maxim Krivokon, Amy Gao, Aditya Joshi, Yu Zhang, Jonathon Shlens, Zhifeng Chen, and Dragomir Anguelov. Scalability in perception for autonomous driving: Waymo open dataset. In *CVPR*, 2020.
- [83] Wouter Van Gansbeke, Simon Vandenhende, Stamatios Georgoulis, and Luc Van Gool. Unsupervised semantic segmentation by contrasting object mask proposals. In *ICCV*, 2021.
- [84] Sara Vicente, Vladimir Kolmogorov, and Carsten Rother. Cosegmentation revisited: Models and optimization. In *ECCV*, 2010.
- [85] Sara Vicente, Carsten Rother, and Vladimir Kolmogorov. Object cosegmentation. In *CVPR*, 2011.
- [86] Antonin Vobecky, David Hurych, Oriane Siméoni, Spyros Gidaris, Andrei Bursuc, Patrick Pérez, and Josef Sivic. Drive&segment: Unsupervised semantic segmentation of urban scenes via cross-modal distillation. *arXiv:2203.11160*, 2022.
- [87] Yangtao Wang, Xi Shen, Shell Hu, Yuan Yuan, James Crowley, and Dominique Vaufreydaz. Self-supervised transformers for unsupervised object discovery using normalized cut. *arXiv:2202.11539*, 2022.
- [88] Mark Weber, Jun Xie, Maxwell Collins, Yukun Zhu, Paul Voigtlaender, Hartwig Adam, Bradley Green, Andreas Geiger, Bastian Leibe, Daniel Cremers, Aljosa Osep, Laura Leal-Taixe, and Liang-Chieh Chen. Step: Segmenting and tracking every pixel. In *NeurIPS Track on Datasets and Benchmarks*, 2021.
- [89] Yunchao Wei, Huaxin Xiao, Honghui Shi, Zequn Jie, Jiashi Feng, and Thomas S. Huang. Revisiting dilated convolution: A simple approach for weakly- and semi-supervised semantic segmentation. In *CVPR*, 2018.
- [90] Yongqin Xian, Subhabrata Choudhury, Yang He, Bernt Schiele, and Zeynep Akata. Semantic projection network for zero-and few-label semantic segmentation. In *CVPR*, 2019.
- [91] Jiarui Xu, Shalini De Mello, Sifei Liu, Wonmin Byeon, Thomas Breuel, Jan Kautz, and Xiaolong Wang. Groupvit: Semantic segmentation emerges from text supervision. *arXiv:2202.11094*, 2022.
- [92] Mengde Xu, Zheng Zhang, Fangyun Wei, Yutong Lin, Yue Cao, Han Hu, and Xiang Bai. A simple baseline for zero-shot semantic segmentation with pre-trained vision-language model. *arXiv:2112.14757*, 2021.
- [93] Chi Zhang, Guankai Li, Guosheng Lin, Qingyao Wu, and Rui Yao. Cyclesegnet: Object co-segmentation with cycle refinement and region correspondence. *IEEE TIP*, 2021.
- [94] Xiao Zhang and Michael Maire. Self-supervised visual representation learning from hierarchical grouping. *NeurIPS*, 2020.
- [95] Hang Zhao, Xavier Puig, Bolei Zhou, Sanja Fidler, and Antonio Torralba. Open vocabulary scene parsing. In *ICCV*, 2017.
- [96] Bolei Zhou, Aditya Khosla, Agata Lapedriza, Aude Oliva, and Antonio Torralba. Learning deep features for discriminative localization. In *CVPR*, 2016.
- [97] Chong Zhou, Chen Change Loy, and Bo Dai. Densclip: Extract free dense labels from clip. *arXiv:2112.01071*, 2021.

Appendices

In this supplementary material, we first discuss broader impact, the role of supervisory signals for ReCo and alternative approaches, and the datasets used in our work (Appendix A). Next we provide further details of experiments conducted in the main paper together with hyperparameters for training ReCo+ in Appendix B. We then report additional ablations investigating the influence of common category selection for context elimination and reducing ambiguity in category name in Appendix C. Finally, we provide additional qualitative results on COCO-Stuff in Sec. D to illustrate both successful and failure cases for our method.

A Discussion of broader impact, supervision and data

A.1 Broader Impact

Semantic segmentation is a *dual use* technology. It enables many applications with the potential for significant positive societal impact across domains in medical imaging, wildlife monitoring, improved fault detection in manufacturing processes etc. However, it is also vulnerable to abuse: it may enable unlawful surveillance or invasions of privacy, for example. By removing the requirement to collect pixel masks for concepts of interests, ReCo lowers the barrier to entry for any individual that wish to make practical use of segmentation, but makes no distinction on the ethical implications of the use case, positive or negative.

ReCo makes use of large-scale, unlabelled image collections. By their nature, such images are subject to minimal curation and sanitisation, and thus may contain not only biases across demographics, but also content that does not align with the ethical values of the user. Consequently, we emphasise that ReCo represents a research proof of concept that is not appropriate for real-world usage without extensive additional analysis of the specific deployment context in which it will be used and, in particular, safeguards to moderate the archive curation process.

A.2 Supervisory signals for ReCo and prior work

In the main paper, we compare to previous methods that are typically described as *unsupervised*. In practice, however, many methods (including ours) either implicitly or explicitly engage humans in the data curation process at some stage.

Supervision used by ReCo. (1) Similarly to prior work, our experiments make use of datasets constructed from photographs taken by humans for both training and evaluation. These photographs are naturally biased towards content that humans find interesting and are typically well-framed (with a concept of interest featuring prominently) or taken from a vantage point that offers a convenient scene overview (e.g. a roof-mounted camera on a vehicle driving on public roads). By training and evaluating on such data, our experimental results likely provide an optimistic assessment of performance when contrasted with other distributions (e.g. the video feed received by an autonomous mobile robot). (2) For our comparisons to prior work, we use the ImageNet training subset without labels to curate archives. However, in practice, this dataset is not free from human involvement: it was curated by human workers who were asked to verify that each image contains a particular synset category (see [16] for a discussion of the collection process). While annotators were encouraged to select images regardless of occlusions, the number of objects and clutter in the scene, this process nevertheless produced a relatively clean dataset with fairly object-centric images. (3) Several of our experiments make use of DeiT-SIN [59], which is trained on stylised ImageNet [20] with labels. We don't believe that this supervision is critical, since in Figure 3 of the main paper, we showed that ResNet50-MoCov2 [25] which does not use labels achieves similar performance (less than 1 mIoU difference on PASCAL-Context [57]). Moreover, we note that previous unsupervised methods to which we compare (e.g. [33, 12]) initialise their approach from supervised ImageNet training with the convention that *unsupervised* in this context denotes the fact that no pixel-level supervision is used. (4) By using CLIP [72], we also make use of a different kind of supervision, namely images paired with alt-text scraped from the web. Empirically, this data source has been shown to be extremely scalable and to enable generalisation to very large numbers of concepts [72, 35, 69]. Nevertheless, the creation of the original alt-text image descriptions (mostly) derives from a human source, and

therefore provides a form of human supervision. In contrast to using ImageNet classification labels, this source of supervision *is* indispensable to ReCo.

We believe that the key factors to be considered when discussing the question of supervision are *scalability* and *generalisation*. We are typically not interested in unsupervised methods for their own sake, but rather because they offer the ability to cheaply scale up machine learning to larger training data sets that improve performance, and to build methods that go beyond the functionality afforded by labelled datasets (e.g. new classes, new tasks etc.). Subject to the caveats (e.g. human photographer bias) outlined above, we believe ReCo has the flexibility to scale up far beyond the experimental comparisons conducted in this work without requiring any changes to the underlying framework.

A.3 Discussion of consent in used datasets

In this work, we work primarily with widely used Computer Vision benchmarks: ImageNet [16], PASCAL-Context [57], Cityscapes [14], COCO-Stuff [6], KITTI-STEP [88]. For these datasets, we do not conduct an independent investigation of consent beyond the considerations of the authors that released these datasets. For our final exploratory studies which make use of LAION-5B [76], we manually verified that no humans were present in the archives that were curated by ReCo.

A.4 Discussion on whether data contains personally identifiable information or offensive content

We do not release any data as part of this work. By working with widely used Computer Vision benchmarks, we also restrict ourselves to imagery that is available in the public domain. We therefore believe that the risk that our work builds on harmful content or contributes to the leakage of personal information is low.

One exception to this is our use of the LAION-5B dataset for qualitative studies. We manually verified that no personally identifiable information or harmful content (as judged by the authors) was present in the archives curated by ReCo.

A.5 Dataset licenses

Here we describe the terms/licenses of datasets used in our paper. For images in PASCAL-Context and COCO dataset, we comply with the Flickr Terms of Use and the Creative Commons Attribution 4.0 License for the COCO-Stuff annotations. For Cityscapes and ImageNet1K, we follow the terms stated on their official website³ and the Attribution-NonCommercial-ShareAlike 3.0 Unported (CC BY-NC-SA 3.0) licence for KITTI-STEP.

B Experiment details

Here we provide pseudocode for ReCo and details of experiments conducted in the main paper.

B.1 Pseudocode for ReCo

In Alg. 1, we describe the pseudocode for the *core* of ReCo (to maintain readability, language-guided co-segmentation and context elimination are omitted since these follow a similar structure).

B.2 Prompt engineering

To obtain the text embedding for a concept, we ensemble the textual features from 85 templates, e.g., “a photo of the {concept}” and “there is a {concept} in the scene” following [97].

³<https://www.cityscapes-dataset.com/license> and <https://www.image-net.org/download.php> for Cityscapes and ImageNet1K respectively.

Algorithm 1 Pseudocode for the core of ReCo (using PyTorch-like syntax)

Input. a CLIP image encoder $\psi_{\mathcal{I}}$, a CLIP text encoder $\psi_{\mathcal{T}}$, an image encoder $\phi_{\mathcal{I}}$, an image collection \mathcal{U} , a concept c , the number of co-segmented images k

Output. a reference image embedding `ref_emb` and a prediction of the concept c in a new image

```
# retrieve images
image_emb = l2_normalize( $\psi_{\mathcal{I}}(\mathcal{U})$ , dim=1) # NxC
text_emb = l2_normalize( $\psi_{\mathcal{T}}(c)$ , dim=0) # C
scores = mm(image_emb, text_emb) # N
indices = argmax(scores)[:k] # k
images =  $\mathcal{U}$ [indices] # kx3xHxW

# co-segment
F = l2_normalize( $\phi_{\mathcal{I}}$ (images), dim=1) # kxCxhxw
F_flat = F.permute(1, 0, 2, 3).view(C, k*h*w) # Cxkhw
A = mm(F_flat.T, F_flat) # adjacency matrix, khwxkhw

grid = zeros((k*h*w, k))
start_col = 0 # start column index
for i in range(k):
    end_col = start_col + h*w # end column index
    grid[:, i] = max(A[:, start_col:start_col+end_col], dim=1)
    start_col = end_col
avg_grid = mean(grid, dim=1) # khw

seed_features = []
start_row = 0 # start row index
for i in range(k):
    end_row = start_row + h*w # end row index
    index_1d = argmax(avg_grid[start_row:end_row])
    start_row = end_row
    index_2d = [index_1d//w, index_1d%w]
    seed_features.append(F[i, :, index_2d[0], index_2d[1]])
seed_features = stack(seed_features, dim=0) # kxC
ref_emb = l2_normalize(seed_features.mean(dim=0), dim=0) # C

# inference
F_new = l2_normalize( $\phi_{\mathcal{I}}$ (new_image), dim=0) # Cxhxw
prediction = sigmoid(mm(ref_emb, F_new)) # hxw
```

mm:matrix multiplication.

B.3 Details of ablation study to assess CLIP retrieval performance

We observe that two of the ImageNet1K class labels are not unique—they occur twice with different meanings (e.g., “crane” is used to represent both bird and machine), which makes retrieval inference and evaluation ambiguous. Therefore, we exclude those classes and use the remaining 996 categories for the experimental results reported in Fig. 3 (left) of the main paper.

B.4 Hyperparameters for ReCo+ training

As described in Sec. 4.2 (in the main paper), we adopt DeepLabv3+⁴ [10] with ResNet101 encoder [26] for ReCo+ and train the network with standard data augmentations such as random scaling and horizontal flip following [61, 79]. In detail, for geometric transformations, we use random scaling with a range of [0.5, 2.0], random crop with a crop size 320×320 pixels, and random horizontal flip with a probability of 0.5. For the photometric augmentations, we apply colour jittering⁵ with 0.8, 0.8, 0.8, 0.2, and 0.8 for brightness, contrast, saturation, hue and probability parameters respectively. We

⁴We use the code for DeepLabv3+ from <https://github.com/VainF/DeepLabV3Plus-Pytorch>.

⁵We use ColorJitter function in `torchvision` package [66].

tree	sky	building	road	person	mIoU
X	X	X	X	X	5.7
✓	X	X	X	X	10.9
✓	✓	X	X	X	12.0
✓	✓	✓	X	X	10.8
✓	✓	✓	✓	X	11.4
✓	✓	✓	✓	✓	12.3

parking →parking lot	vegetation →tree	mIoU
X	X	15.4
X	✓	16.0
✓	X	18.6
✓	✓	19.3

Table 3: **Effect of context category choices and reducing label ambiguity.** **Left:** We find that suppressing 5 frequently appearing categories brings performance gain on PASCAL-Context [57]. **Right:** We observe that specifying the meaning of a class more concretely helps segmentation performance of ReCo on Cityscapes [14].

also employ Gaussian blurring with a kernel size of 10% of $\min(H, W)$ where $\min(H, W)$ returns the length of the shorter side of an image.

C Additional ablation studies

C.1 Choices of context categories

As described in Sec. 3.2 (main paper), we propose to suppress the commonly appearing categories, *e.g.*, *sky*, which co-occur with other classes, *e.g.*, *aeroplanes*. To achieve this, we manually pick 5 frequently appearing classes in PASCAL-Context dataset [57] and investigate the effect of different combinations of such categories. In Tab. 3 (left) we observe that suppressing the *tree* and *sky* categories yields a notable performance gain, while eliminating all five categories performs best. For this reason, we apply the context elimination strategy with these five categories in the main paper.

C.2 Category name rephrasing to reduce ambiguity

We observe that it is important to specify a concept concretely to obtain retrieved images exhibiting similar visual appearance. For instance, in Cityscapes dataset, *parking* and *vegetation* can be rephrased to less ambiguous concepts *parking lot* and *tree* respectively based on their descriptions⁶ in the paper accompanying the dataset [14]. As can be seen in Tab. 3 (right), ReCo gains benefits in performance on Cityscapes by replacing the category names with less abstract concepts. This sensitivity is a consequence of our co-segmentation algorithm, which locates pixels that share similar visual features across multiple images. Thus we use the rephrased label names throughout the experiments in the paper.

In addition to the limitations listed in the main paper, this dependence on concrete/specific concept names can be considered a limitation of our approach (albeit one that is readily mitigated). However, we believe it is a reasonable requirement for methods that operate in the zero-shot transfer setting. Unlike fine-tuning methods that learn to associate abstract text descriptions to visual concepts by seeing examples from the target distribution, ReCo relies entirely on an adequate text description to disambiguate the concept. Since many computer vision datasets have been constructed with training and testing splits with the assumption that methods would *make use of the training set*, we believe it is probable that category names were not designed to be uniquely descriptive (hence the use of “parking” as a category in Cityscapes, which could be either a verb or a noun). Indeed, there may have been little perceived need to construct unambiguous category names when examples from the training set implicitly provide disambiguation of the concept.

⁶“Horizontal surfaces that are intended for parking and separated from the road, either via elevation or via a different texture/material, but not separated merely by markings.” for *parking* and “Trees, hedges, and all kinds of vertically growing vegetation.” for *vegetation*.

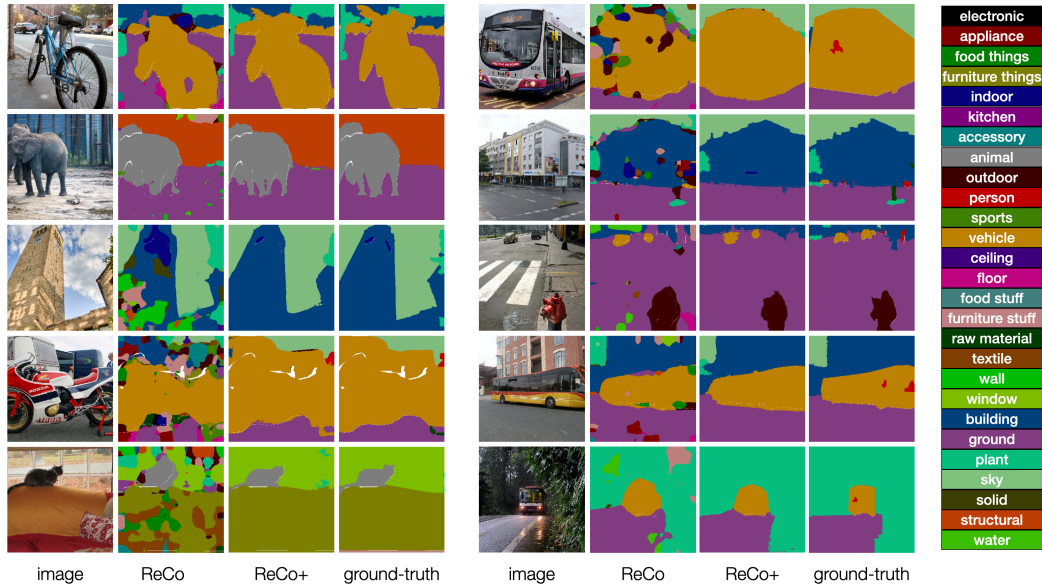


Figure 5: **Additional visualisations on COCO-Stuff.** **Left:** Successful cases. **Right:** Typical failure cases. White pixels denote ignored regions.

D Additional visualisations

In Fig. 5, we show more visualisation samples on COCO-Stuff benchmark. Successful and failure cases are shown on the left and right, respectively. We note that ReCo tends to fail in predicting small objects, *e.g.*, people in the bus, and so does ReCo+ which is trained on the ReCo’s predictions as pseudo-labels. We conjecture that this is related to the stride of the image encoder used for ReCo, which is 16×16 for the case of DeiT-S/16-SIN [59]. It could therefore potentially be improved by using an encoder with a smaller stride at the cost of increased computational burden.